

Numerical and Experimental Study of the Optimal Location of Concrete Piles in a Saturated Sandy Slope

Mohammad Hajiazizi¹ · Moslem Bavali¹ · Ali Fakhimi²

Received: 8 July 2016 / Revised: 16 January 2017 / Accepted: 20 January 2017 / Published online: 16 February 2017
© Iran University of Science and Technology 2017

Abstract The stability of a soil slope, reinforced by a concrete pile, is studied both experimentally and numerically in this work. Our study suggests that when the concrete pile is located in the middle of the slope (at $x/r=0.5$), the soil structure collapses under a pressure of 10.9 kPa that is the highest overburden pressure to cause instability of the tested reinforced sandy slope. However, when the pile is located in the upslope (at $x/r=0.75$) or downslope (at $x/r=0.25$), the slope failure occurs under a pressure of 7.8 or 3.12 kPa, respectively. Therefore, our experimental work suggests that a pile located at the middle of the slope can provide the optimum reinforcement of the soil structure studied in this work. The nonlinear numerical modeling of the slope was conducted as well. The numerical study shows consistent results with those from the physical observation confirming that the slope mid-point is the optimum place for the slope reinforcement.

Keywords Slope reinforcement · Optimal pile location · Concrete pile · Sandy slope

1 Introduction

When instability of an earth slope is a possibility, it is imperative to take preventive measures before instability can actually occur. What should be considered at the beginning of any stabilization process is the minimization of the cost while the factor of safety is improved. The first simple possible step to maintain the stability of an earth slope is to perform excavation of the slope crest or/and filling in the slope toe. If these techniques are not feasible or do not provide the required factor of safety, it will be necessary to use other stabilization methods such as increasing the soil strength parameters, draining the surface and subsurface water, and installing retaining walls and piles. These solutions are aimed at mitigating the driving forces and/or increasing the resistive forces. To evaluate the appropriateness of the supporting elements in an earth slope, analytical, numerical, and experimental methods are normally utilized. Modeling the stability of earth slopes using numerical methods is a common practice in geotechnical engineering.

One of the methods used for improving resistive forces is the installation of concrete piles in earth slopes. Poulos [1] implemented the LE (limit equilibrium) method to assess stabilization of earth slopes using piles. He concluded that the optimal location for the pile installation is near the center of the wedge which has the failure potential. Other researchers [2] introduced a simple approach for analysis of the effect of a row of piles for stabilization of earth slopes. The suggested approach in [2] is based on a non-coupling formulation, which considers pile response and slope sustainability, separately. In this analysis, shear forces and bending moments resulting from lateral movement of soil mass are calculated using the modified boundary element method [3]. The developed friction circle method

✉ Mohammad Hajiazizi
mhazizi@razi.ac.ir

Moslem Bavali
moslem.bavali@yahoo.com

Ali Fakhimi
ali.fakhimi@nmt.edu

¹ Department of Civil Engineering, Razi University, Taq-e Bostan, Kermanshah, Iran

² Department of Mineral Engineering, New Mexico Institute of Mining and Technology, Socorro, NM, USA

and the methods of Ito and Matsui [4], Ito et al. [5], and Ito et al. [6] were used in [7] to indicate that piles should be near the slope crest in order to obtain the maximum factor of safety. The work reported in [8] utilized the three-dimensional FE method to prove that the maximum factor of safety is achieved by locating the piles at the center of the slope. A kinematical limit analysis approach was utilized in [9] for the analysis of the stability of earth slopes. The authors showed in [9] that since the force required by the pile to support the slope is at its minimum level near the toe, the best location to install the pile is near the toe. The application of FLAC3D software suggested that the best location to install a pile is in the middle of the slope; the pile receives the highest pressure at this location [10]. The limit analysis carried out in [11] revealed that the optimal location for installation of a retaining pile is near the toe. This is because forces required to increase the factor of safety are minimum at or near the toe. The work reported in [12] modeled a slope reinforced by a row of piles using the FLAC3D software. They realized that the optimal locations for pile installation in a sandy soil and a clayey soil are in the middle of the slope and near the crest, respectively. They also indicated that when the slope is made of a sandy soil, shallow failure occurs along the slope surface, which starts from the vicinity of the crown. Therefore, the center of the failure surface approaches the middle of the slope and the optimal location for the pile installation is near the middle of the slope. However, when the slope is made of clay, deep failure occurs in the slope and the failure surface lies far from the crest. Consequently, the distance between the center of the failure surface and the middle of the slope increases and the optimal pile location lies far from the middle of the slope.

Stabilization analysis of earth slopes has been divided into the following two categories: (1) displacement- or pressure-based methods and (2) numerical methods [13]. In [13], a hybrid methodology, for the design of slope-stabilizing piles, was suggested. The method combines the rigor of 3D finite element simulation with the simplicity of widely accepted analytical techniques. The piles with distance equal to $5D$ (D is the pile diameter) are embedded in the stable soil because the zone of influence of each pile has been demonstrated not to exceed $5D$. The length of each pile is restricted to $10D$ in the suggested method. The work reported in [14] optimized the pile location using a combination of limit analysis method and theories proposed in [4–6]. In [14], it was attempted to calculate the lateral load imposed on a pile and concluded that the most effective location for pile installation is near the slope toe where the pile carries the minimum force for achieving the required factor of safety. A new micro-pile design method for earth slope stabilization

that includes details about choosing the location for the micro-piles within the existing slope and selecting the micro-pile cross-sectional area was suggested in [15]. The results of field tests on a single laterally loaded pile and two piles in line, and bored reinforced concrete piles with a diameter of 0.25 m and a depth of 5 m that were constructed in a natural sandy gravel soil, were reported in [16]. Askarinejad [17] studied the effects of pore water pressure perturbations on the stability of unsaturated silty sand slopes. Hajiazizi and Mazaheri [18] used line segment slip surface for optimized design of piles in stabilization of earth slopes. Either 2D or 3D methods can be used to obtain the critical slip surface of a slope [19]. Additional work regarding the soil reinforcement, reinforced concrete column, and interaction between soil and rock with a supporting structural system can be found in [20–25].

Previous studies discussed above suggest that there is no consensus about the optimal location of a retaining pile within a slope. A reliable approach to obtain the best location for a retaining wall is to conduct physical tests that are accompanied by numerical modeling. This is the objective of the present paper. A sandy soil slope was constructed in the laboratory and then was gradually loaded by the process of saturation through precipitation. Several soil slopes were tested and the effect of the location of the retaining pile on the slope stability was investigated. The nonlinear finite element method using the PLAXIS computer program [26] was conducted as well to model the experimental findings and observations.

2 Specimen and Equipment

The box used for the slope stability tests is shown in Fig. 1. It has a length of 180 cm, a height of 60 cm, and a width of 20 cm. In order to avoid the additional resistance contributed by the box, its walls were lubricated before building the model. Moreover, high-resolution camcorders were used to record all events.

The slope built in the laboratory has a height of 30 cm and is made of a sandy soil. The unit weight of the soil is 18 kN/m^3 . According to the direct shear tests performed on the sand samples, the angle of friction for the saturated soil is 36 degrees and that for the dry soil is 46 degrees. Soil cohesion was about 0.002 MPa which was ignored in our analysis. The particle size distribution curve for the sand is depicted in Fig. 2. In order to stabilize the slope, concrete piles were employed (Fig. 3). The concrete pile was located between the slope toe and crest (at different x/r values) as shown in Fig. 4.

Fig. 1 The *box* used for the tests and the piezometric panel

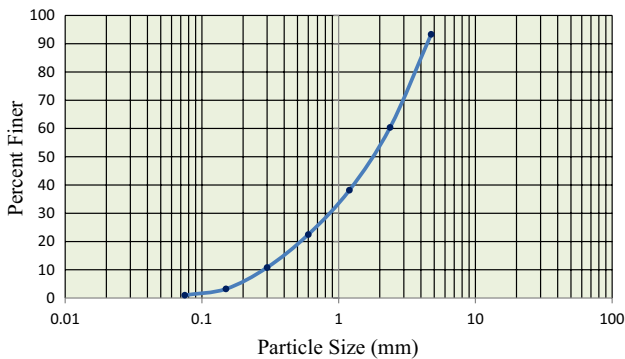


Fig. 2 Particle size distribution curve

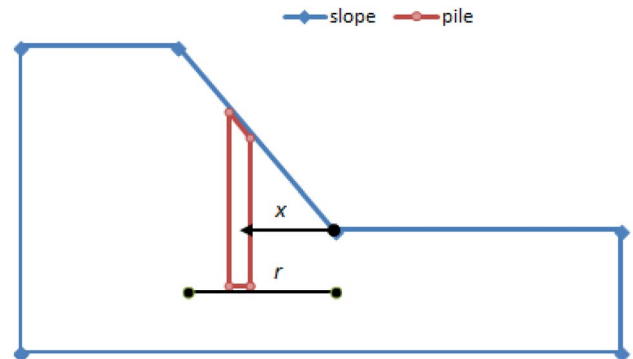


Fig. 4 Location of the pile between the toe and the crown measured by x/r ratios



Fig. 3 Concrete piles used at different locations along the slope

3 Experimental and Numerical Modeling

The tested slopes are made of a sandy soil described before. The testing scenarios are as follows: (1) a slope without a concrete pile, (2) a slope reinforced with an upstream concrete pile, (3) a slope reinforced with a downstream concrete pile, and (4) a slope reinforced with an intermediary concrete pile. The diameter of the concrete pile is 3.6 cm and its tip reaches near the box floor. The overall geometry of the physical test set-up is shown in Fig. 5.

Precipitation was provided using a sprinkler system installed at the top of the slope which is depicted in Fig. 5. The flow velocity was 2 L/min. The testing box was provided with drainage. In other words, on the slope downstream, a drain was installed to allow for drainage of the water.

The pore water pressure on the slope was measured using a piezometric panel. The piezometric panel is composed of 14 piezometer pipes used to measure pore water



Fig. 5 Slope made of sand with a slope angle of 45°

pressure at different points along the base of the slope (Fig. 6). The piezometric water level increased over time during precipitation until the soil was saturated. It is worth mentioning that in all models soil failure occurred following saturation and no crack or failure was observed before saturation.

The slope was compacted and built in the dry state. Therefore, the initial pore pressure was zero. Following the construction of the earth slope, artificial rain was induced and pore water pressure increased gradually. Variations of pore water pressure were measured using the piezometers.

The following three positions were selected for pile installation: $x/r=0.25$ (downslope), $x/r=0.5$ (middle), and $x/r=0.75$ (upslope).

3.1 Model 1: Slope Without Concrete Pile

In this section, the stability of the slope (Model 1) is investigated without using the concrete pile. The slope was compacted and built in the dry state. The sand was compacted with a unit weight of 18 kN/m³. In order to compact the sand in the experimental tank and obtain the desired unit weight, a checkered pattern was created in the experimental tank; based on the volume of each of the blocks in the tank, the required weight of sand was obtained to achieve a unit weight of 18kN/m³. Finally, the calculated weight of sand was poured and compacted to reach the desired specified volume.

As described before, the model was subjected to artificial precipitation. Following the addition of water, the slope experienced failure after 50 min (Fig. 7). In fact, after 50 min, the soil was saturated completely and its air content was minimized. The time–water level diagram for piezometers #1 to #4 (Fig. 6) is shown in Fig. 8. In order to assess the instability of the slope, Model 1 was also numerically

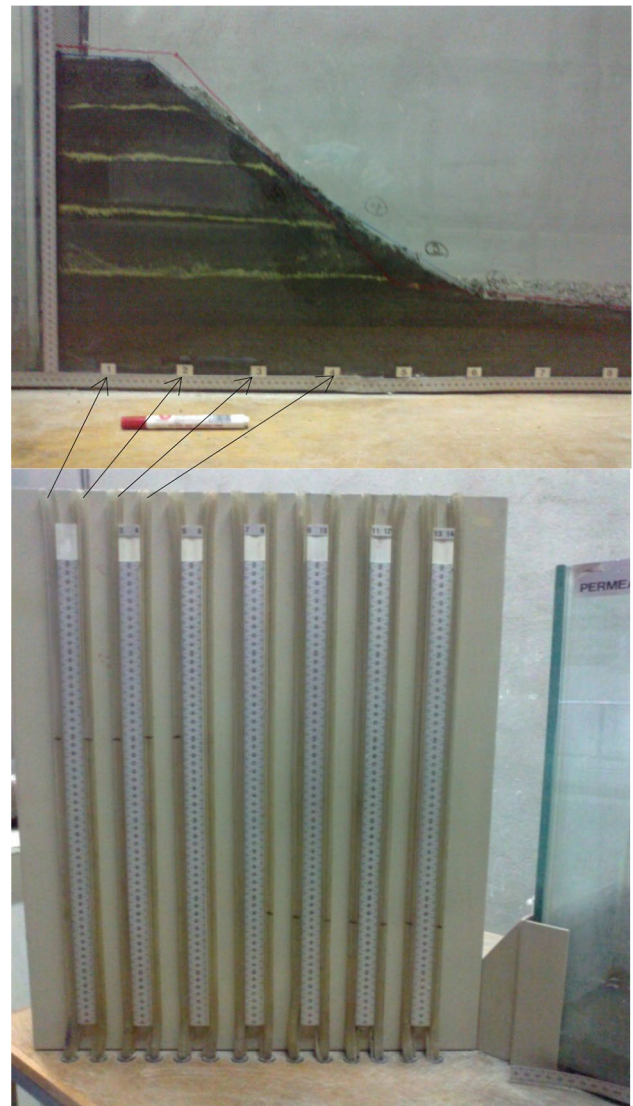


Fig. 6 Fourteen piezometric pipes for measuring the water level at different points



Fig. 7 Slope failure after 50 min (model 1)

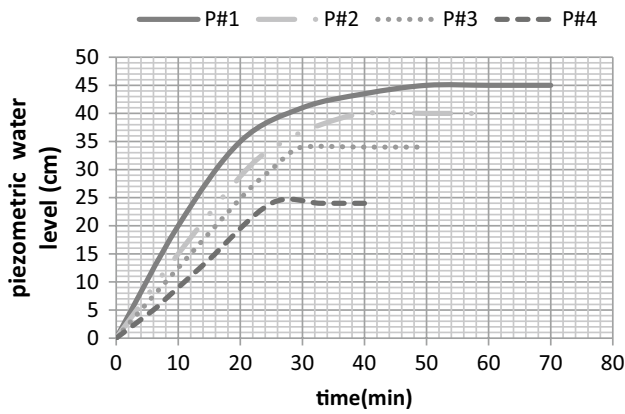


Fig. 8 Variation of piezometric water level with time for piezometers #1–#4

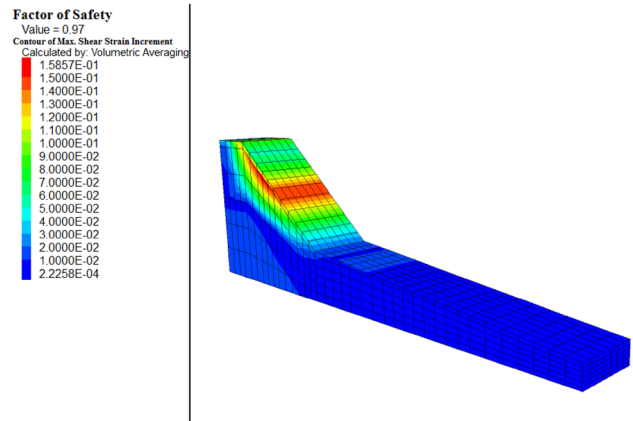


Fig. 10 Contours of shear strain increment in the slope. Note that the maximum shear strain increment occurred in the middle of the slope

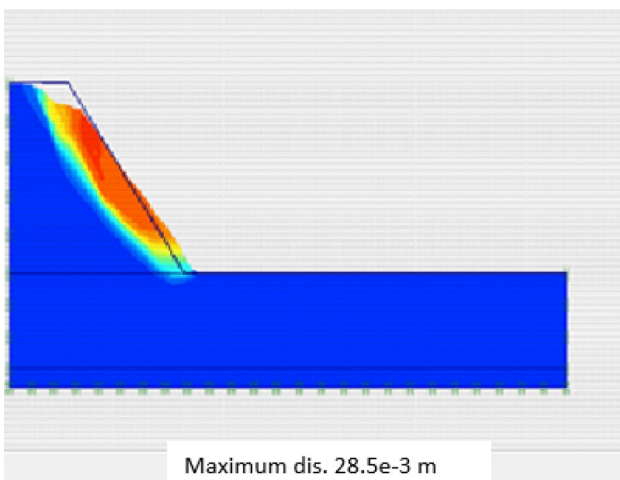


Fig. 9 Stability analysis using the FE method ($FS_{min} = 0.85$)

Table 1 Properties of soil in numerical modeling

Parameters	Value
Sand dry unit weight	18 KN/m ³
Sand saturated unit weight	20 KN/m ³
Sand bulk modulus	3.3×10^7 N/m ²
Sand shear modulus	1.5×10^7 N/m ²
Sand cohesion	2 kPa
Sand friction angle in dry condition	46°
Sand friction angle in saturated condition	36°

simulated using the FE method (Fig. 9). The physical properties of the soil, which were used for the numerical analysis, are reported in Table 1; the elastic properties were just estimated. Note that the soil elastic properties have no or negligible effect on the safety factor as in LE methods they are not needed at all. A Mohr–Coulomb plasticity model

was utilized for the stability analysis. In the numerical modeling, triangular elements with 15 nodes were used. Both vertical boundaries are fixed in the x-direction and the horizontal bottom boundary is fixed in both x- and y-directions.

The value of the factor of safety resulting from the FE method is 0.85. The value of factor of safety is smaller than 1, which is consistent with the physical observation reflecting the instability of the slope. Note that, following the saturation condition, the maximum shear deformation increment occurred in the middle of the slope (Fig. 10). This suggests that to prevent and control the excessive deformation of the soil structure, the pile should be placed in the middle of the slope.

3.2 Model 2: Slope Reinforced with Upslope Concrete Pile

In this model, the concrete pile is installed in the slope upstream (at $x/r=0.75$) (Fig. 11). The length, diameter, and unit weight of the concrete pile are 36.4 cm, 3.6 cm, and 25 kN/m³, respectively. The distance between the pile tip and the box floor is 3.6 cm.

In order to build the reinforced slope, the pile was first placed at the desired location and then the earth slope was constructed. This is to make sure that the slope is supported by the concrete pile and no premature failure has occurred. The slope was subjected to artificial precipitation for 100 min, during which no fracture or crack was observed in the slope. If the slope was subjected to even more than 100 min of precipitation, it would not fail. Note that the stability of the reinforced slope was confirmed by the FE method ($FS = 1.20$) as well. Following slope saturation, the slope was subjected to gradual loading to see when it would fail. Following the gradual loading on the crown, the slope failed under a pressure

Fig. 11 A concrete pile with a diameter of 3.6 cm installed at $x/r=0.75$



Fig. 12 Slope failed under a pressure of 7.8 kPa (Model 2)

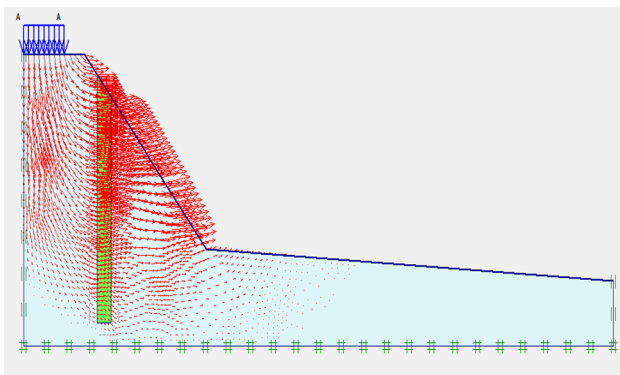


Fig. 13 Failure of Model 2 after loading: FE method with an applied overburden pressure of 7.2 kPa

of 7.8 kPa (Fig. 12). The saturated slope with the applied pressure was analyzed using the FE method. In the FE method, with an applied pressure of 7.2 kPa the factor of safety was reduced to less than 1 (Fig. 13). Note that the overburden pressures to cause failure in the physical and numerical simulations of Model 1 show close agreement.

3.3 Model 3: Slope Reinforced with Downstream Concrete Pile

In this model, a concrete pile with a diameter of 3.6 cm is installed in the slope downstream (at $x/r=0.25$). After installing the concrete pile in its position and construction of the soil structure, the slope was saturated through precipitation.

The length, diameter, and unit weight of the concrete pile are 16.4 cm, 3.6 cm, and 25 kN/m³, respectively. The distance between the pile tip and the box floor is 3.6 cm. The slope was subjected to artificial precipitation for 100 min. In this period, no fracture or crack was observed in the slope. The FE result was consistent with the experimental findings (FS = 1.10) suggesting no slope failure. Following slope precipitation, the slope was subjected to gradual loading to see when it would fail. After gradual loading on the crown, the slope failed under a pressure of 3.12 kPa. The value of critical pressure (for failure due to loading) obtained using the FE method after performing the stability analysis of Model 3 is 3 kPa. This is in close agreement with the critical overburden pressure from the physical test. Figure 14 shows the failure pattern obtained by the FE analysis.

3.4 Model 4: Slope Reinforced with Intermediary Concrete Pile

In this model, the concrete pile is located in the middle of the slope (at $x/r=0.5$). The length, diameter, and unit weight of the concrete pile are 26.4 cm, 3.6 cm, and 25 kN/m³, respectively. The distance between the pile tip and the box floor is 3.6 cm. The slope was subjected to artificial precipitation for 100 min. In this period, no fracture or crack was seen in the slope. The physical test result was consistent with that observed from the FE method; the finite element method suggested a factor of safety greater than one (FS = 1.44). Subsequently, the slope was subjected to gradual loading to see when it collapses. After gradual

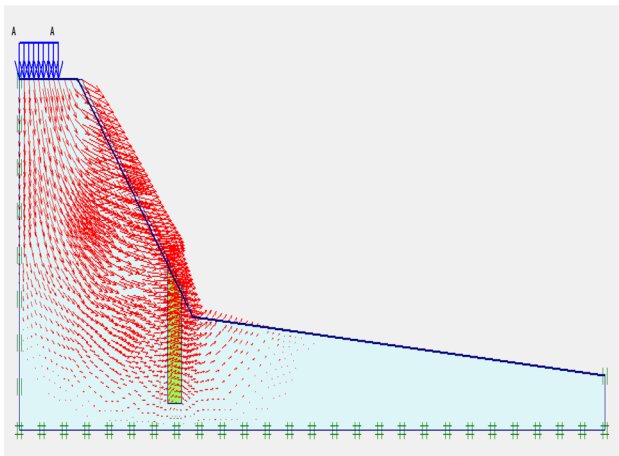


Fig. 14 Failure of Model 3 after loading: FE method with an applied overburden pressure of 3 kPa

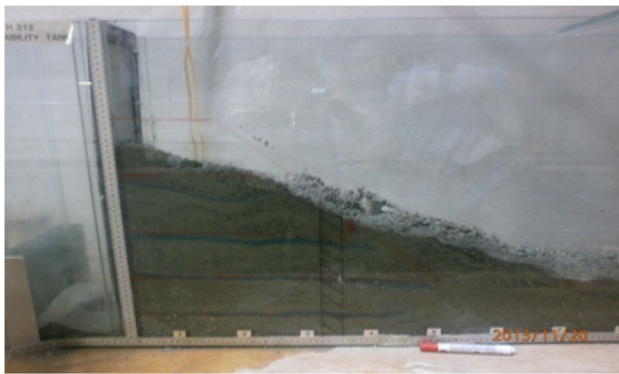


Fig. 15 Failure of the soil slope under a pressure of 10.9 kPa (Model 4). The pile is located in the middle part of the slope

loading on the crown, the slope failed under a pressure of 10.9 kPa (Fig. 15). The value obtained for the critical pressure using the FE method is 9.3 kPa. This numerical value of minimum pressure required for failure of the slope is in close agreement with that of the experimental test. Figure 16 shows the result of slope stability analysis using the FE method.

4 Dimensional Analysis

Scale or size effect is an important subject in structural mechanics [27]. Dimensional analysis can be applied to extend the experimental results to the field situation using Table 2, in which *S* is the scaling parameter. Therefore, using Table 2, we may convert the results of an experimental model into a real full-scale one. It should be noted that soil characteristics, such as cohesion, angle of internal

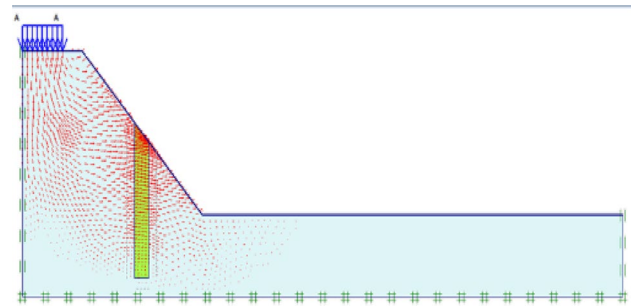


Fig. 16 Failure of Model 4 after loading; induced deformation predicted by the FE method with an applied overburden pressure of 9.3 kPa

friction, and soil unit mass, normally remain fixed in both real and experimental models after scaling. For example, a slope with a height of 30 cm and an angle of 45 degrees in the experimental test is equivalent to a slope with a height of 30 m and an angle of 45 degrees in nature based on a scale ratio $S = 1/100$. These differences occur because of differences in stress level between the model tests and field tests [28]. With regard to this issue, Sawwaf [29] proposed that 1-g models can be useful only in the prediction of general behaviors of prototypes. In this regard, other researchers [30] explained that small-scale 1-g model tests help approximate information about the general behavior of the prototypes quicker and simpler than the large-scale tests. However, the large-scale tests have better control over key parameters of the model. It should be noted that the results of small-scale tests are affected by scale effects and the results obtained from 1-g models are not directly applicable to the prototype. As proposed by a few researchers [31], the results of the small-scale tests can be extrapolated to prototype by applying scaling law carefully. They also showed that it is not possible to create completely similar conditions for model and prototype due to the involvement of several complex factors and it should be left to the judgment of the researchers to decide about these influencing factors. According to the items listed above and Sawwaf [29], it is recommended to carry out further investigations using large-scale tests or centrifuge model tests in order to better verify the results of this study.

Table 2 Scaling method to convert the experimental model results to a full-scale field problem

	Time	Length	Area	Force	Mass
Real	<i>T</i>	<i>L</i>	<i>A</i>	<i>F</i>	<i>M</i>
Experimental model	$\sqrt{S}T$	<i>LS</i>	<i>AS</i> ²	<i>S</i> ² <i>F</i>	<i>S</i> ³ <i>M</i>

The scaling factor is *S*

Table 3 Values of FS_{\min} (minimum safety factor) resulted from the FE analysis of saturated slope

Location of pile	Laboratory test	FE method
Without pile	Unstable	0.85
$x/r=0.75$	Stable	1.20
$x/r=0.25$	Stable	1.10
$x/r=0.5$	Stable	1.44

5 Discussion of the Results

In this paper, experimental tests were carried out for the stability analysis of sandy slopes reinforced by concrete piles. The purpose of the experimental investigation was to help resolve the discrepancy in the literature regarding the best place for installation of a reinforcing pile. In addition, numerical modeling was implemented for stability analysis of the slopes. The experimental results show that the studied unreinforced sandy slope fails if it is saturated (Table 3) and that it can become stable by installing a concrete pile within the soil structure. Both the numerical and the experimental test results suggest that irrespective of the location of the concrete pile, slope failure can be controlled for this particular soil slope against soil saturation. This does not mean that the same safety factor is obtained irrespective of the pile location. To investigate this issue, following soil saturation, a uniform overburden pressure was applied at the slope top to check the resilience of the reinforced soil slope against further external disturbances. Both the physical tests and the numerical models suggest that the highest overburden pressure to cause instability of the tested reinforced sandy slope following its full saturation is achieved if the pile is installed in the middle part of the slope (Table 4). Note that the numerical models proposed by some other researchers [8, 10, 12] also have suggested the middle of the slope as the best location for the pile to achieve the highest safety factor.

Inspection of the slope deformation in the numerical modeling indicates that maximum incremental shear deformation occurs in the middle of the slope. To control this excessive deformation, a retaining structure is needed. By installing the pile in the middle of the slope, the greatest factor of safety is achieved, while the deformation of the soil slope is restrained and controlled more effectively.

It is interesting to note that the physical and numerical overburden pressures show close agreement (Table 4), suggesting that the proposed numerical model is a reliable technique in the study of the stability of reinforced slopes. It is important to realize that the conclusions of this paper are only applicable when stability and reinforcement of sandy slopes are involved. Physical testing is required

Table 4 Minimum overburden pressure required for failure of the slope

Location of pile	Laboratory test (kPa)	FE method (kPa)
$x/r=0.75$	7.80	7.2
$x/r=0.25$	3.12	3.0
$x/r=0.5$	10.90	9.3

to investigate the situation when cohesive materials are involved.

6 Conclusion

In this paper, numerical and experimental tests were carried out for stability analysis of sandy slopes reinforced by concrete piles. In Model 1 (slope without a concrete pile), the slope was subjected to artificial precipitation. Following the addition of water, the slope experienced failure after about 50 min. In Model 2 (slope reinforced with an upslope concrete pile), following slope saturation, the slope was subjected to gradual loading on the crown, and it failed under a pressure of 7.8 kPa. In Model 3 (slope reinforced with a downstream concrete pile), following slope precipitation, the slope was subjected to gradual loading. After gradual loading on the crown, the slope failed under a pressure of 3.12 kPa. In Model 4 (slope reinforced with intermediary concrete pile), after gradual loading on the crown, the slope failed under a pressure of 10.9 kPa. Accordingly, the best location to install a pile is in the middle of the slope. Both the numerical and the physical test results suggest that the maximum overburden pressure can be carried by the reinforced slope if the pile is installed in the middle ($x/r=0.5$) of the slope.

Installation of the pile in the middle part of the slope not only results in the maximum factor of safety of the structure, but also it helps control the excessive deformation of the mid-slope. The mid-slope excessive deformation could be an indication of shear band formation that can be followed by sudden failure of the slope. The experimental and numerical findings reported in this paper should remove the discrepancy in the literature regarding the optimum location for installation of a pile in a sandy slope.

References

1. Poulos HG (1995) Design of reinforcing piles to increase slope stability. *Can Geotech J* 32(5):808–818. doi:10.1139/t95-078
2. Lee CY, Hull TS, Poulos HG (1995) Simplified pile-slope stability analysis. *Comput Geotech* 17:1–16. doi:10.1016/0266-352X(95)91300-S

3. Hull TS, Lee CY, Poulos HG (1991) Mechanics of pile reinforcement for unstable slopes. Research Report No. 636, School of Civil and Mining Engineering, University of Sydney, Australia
4. Ito T, Matsui T (1975) Methods to estimate lateral force acting on stabilizing piles. *Soils Found* 15:43–59. doi:[10.3208/sandf1972.15.4_43](https://doi.org/10.3208/sandf1972.15.4_43)
5. Ito T, Matsui T, Hong WP (1979) Design method for the stability analysis of the slope with landing pier. *Soils Found* 19(4):43–57. doi:[10.3208/sandf1972.19.4_43](https://doi.org/10.3208/sandf1972.19.4_43)
6. Ito T, Matsui T, Hong WP (1981) Design method for stabilizing piles against landslide one row of piles. *Soils Found* 21(1):21–37. doi:[10.3208/sandf1972.21.21](https://doi.org/10.3208/sandf1972.21.21)
7. Hassiotis S, Chameau JL, Gunaratne M (1997) Design method for stabilization of slopes with piles. *J Geotech Geoenviron Eng ASCE* 123(4):314–323. doi:[10.1061/\(ASCE\)1090-0241](https://doi.org/10.1061/(ASCE)1090-0241)
8. Cai F, Ugai K (2000) Numerical analysis of the stability of a slope reinforced with piles. *Soils Found* 40(1):73–84. doi:[10.3208/sandf.40.73](https://doi.org/10.3208/sandf.40.73)
9. Ausilio E, Conte E, Dente G (2001) Stability analysis of slopes reinforced with piles. *Comput Geotech* 28:591–611. doi:[10.1061/40863\(195\)8](https://doi.org/10.1061/40863(195)8)
10. Won J, You K, Jeong S, Kim S (2005) Coupled effects in stability analysis of pile-slope systems. *Comput Geotech* 32:304–315. doi:[10.1016/j.compgeo.2005.02.006](https://doi.org/10.1016/j.compgeo.2005.02.006)
11. Nian TK, Chen GQ, Luan MT, Yang Q, Zheng DF (2008) Limit analysis of the stability of slopes reinforced with piles against landslide in nonhomogeneous and anisotropic soils. *Can Geotech J* 45(8):1092–1103. doi:[10.1139/T08-042](https://doi.org/10.1139/T08-042)
12. Wei WB, Cheng YM (2009) Strength reduction analysis for slope reinforced with one row of piles. *Comput Geotech* 36:1176–1185. doi:[10.1016/j.compgeo.2009.05.004](https://doi.org/10.1016/j.compgeo.2009.05.004)
13. Kourkoulis R, Gelagoti F, Anastasopoulos I, Gazetas G (2012) Hybrid method for analysis and design of slope stabilizing piles. *J Geotech Geoenviron Eng* 138(1):1–14. doi:[10.1061/\(ASCE\)GT.1943-5606.0000546](https://doi.org/10.1061/(ASCE)GT.1943-5606.0000546)
14. Xinpo Li, Xiangjun P, Marte G, Siming H (2012) Optimal location of piles in slope stabilization by limit analysis. *Acta Geotech* 7:253–259. doi:[10.1007/s11440-012-0170-y](https://doi.org/10.1007/s11440-012-0170-y)
15. Sun SW, Zhu BZ, Wang JC (2013) Design method for stabilization of earth slopes with micropiles. *Soils Found* 53(4):487–497. doi:[10.1016/j.sandf.2013.06.002](https://doi.org/10.1016/j.sandf.2013.06.002)
16. Jagodnik V, Arbanas Z (2015) Testing of laterally loaded piles in natural sandy gravels. *Int J Phys Model Geotech* 15(4):191–208. doi:[10.1680/jphmg.14.00010](https://doi.org/10.1680/jphmg.14.00010)
17. Askarinejad A (2013) Failure mechanisms in unsaturated silty sand slopes triggered by rainfall. Ph.D thesis for doctor of sciences, No. 21423, ETH Zurich
18. Hajiazizi M, Mazaheri AR (2015) Use of line segments slip surface for optimized design of piles in stabilization of the earth slopes. *Int J Civil Eng* 3(1):14–27
19. Hajiazizi M, Tavana H (2013) Determining three-dimensional non-spherical critical slip surface in earth slopes using an optimization method. *Eng Geol* 153:114–124
20. Heidarzadeh M, Mirghasemi AA, Sadr Lahijani SM (2013) Application of cement grouting for stabilization of coarse materials. *Int J Civil Eng* 1(11):71–77
21. Nazari Afshar J, Ghazavi M (2014) A simple analytical method for calculation of bearing capacity of stone-column. *Int J Civil Eng* 1(12):15–25
22. Mosallanezhad M, Sadat Taghavi SH, Hataf N, Alfaro MC (2016) Experimental and numerical studies of the performance of the new reinforcement system under pull-out conditions. *Geotext Geomembr* 44:70–80. doi:[10.1016/j.geotextmem.2015.07.006](https://doi.org/10.1016/j.geotextmem.2015.07.006)
23. Mosallanezhad M, Alfaro MC, Hataf N, Sadat Taghavi SH (2016) Performance of the new reinforcement system in the increase of shear strength of typical geogrid interface with soil. *Geotext Geomembr* 44(3):457–462. doi:[10.1016/j.geotextmem.2015.07.005](https://doi.org/10.1016/j.geotextmem.2015.07.005)
24. Sadeghi K (2017) Nonlinear numerical simulation of reinforced concrete columns under cyclic biaxial bending moment and axial loading. *International Journal of Civil Engineering* 15(1):113–124. doi:[10.1007/s40999-016-0046-x](https://doi.org/10.1007/s40999-016-0046-x)
25. Yang F, Cao S, Qin G. (2017) Performance of the prestressed composite lining of a tunnel: case study of the Yellow river crossing tunnel. *Int J Civil Eng*. doi:[10.1007/s40999-016-0124-0](https://doi.org/10.1007/s40999-016-0124-0)
26. Plaxis Company (2003) Geotechnical software, PLAXIS 2D V.8. Netherland
27. Harris HG, Sabnis G (1999) Structural modeling and experimental techniques, 2nd edn. CRC, New York
28. Vesic AS (1973) Analysis of ultimate loads of shallow foundations. *J Soil Mech Found* 99(1):45–73. doi:[10.1016/0148-9062\(74\)90598-1](https://doi.org/10.1016/0148-9062(74)90598-1)
29. Sawwaf M (2015) Strip footing behavior on pile and sheet pile-stabilized sand slope. *J Geotech Geoenviron Eng ASCE* 131(6):705–715. doi:[10.1061/\(ASCE\)1090-0241\(2005\)131](https://doi.org/10.1061/(ASCE)1090-0241(2005)131)
30. Hegde AM, Sitharam TG (2015) Experimental and numerical studies on protection of buried pipe line sand underground utilities using geocells. *Geotext Geomembr* 43(5):372–381. doi:[10.1016/j.geotextmem.2015.04.010](https://doi.org/10.1016/j.geotextmem.2015.04.010)
31. Fakhre A, Jones CJFP (2009) Discussion on bearing capacity of rectangular footings on geogrid reinforced sand by Yetimoglu T, Wu JTH, Saglamer A 1994. *J Geotech Eng* 122:326–327